Accepted Manuscript

β-amino alcohols and their respective 2-phenyl-N-alkyl aziridines as potential DNA minor groove binders

Miguel M. Vaidergorn, Zumira A. Carneiro, Carla D. Lopes, Sérgio de Albuquerque, Felipe C.C. Reis, Sofia Nikolaou, Juliana F.R. Mello, Giovani L. Genesi, Gustavo H.G. Trossini, A. Ganesan, Flavio S. Emery

PII: S0223-5234(18)30620-2

DOI: 10.1016/j.ejmech.2018.07.055

Reference: EJMECH 10590

To appear in: *European Journal of Medicinal Chemistry*

Received Date: 28 May 2018

Revised Date: 17 July 2018

Accepted Date: 23 July 2018

Please cite this article as: M.M. Vaidergorn, Z.A. Carneiro, C.D. Lopes, Sé. de Albuquerque, F.C.C. Reis, S. Nikolaou, J.F.R. Mello, G.L. Genesi, G.H.G. Trossini, A. Ganesan, F.S. Emery, β-amino alcohols and their respective 2-phenyl-N-alkyl aziridines as potential DNA minor groove binders, *European Journal of Medicinal Chemistry* (2018), doi: 10.1016/j.ejmech.2018.07.055.

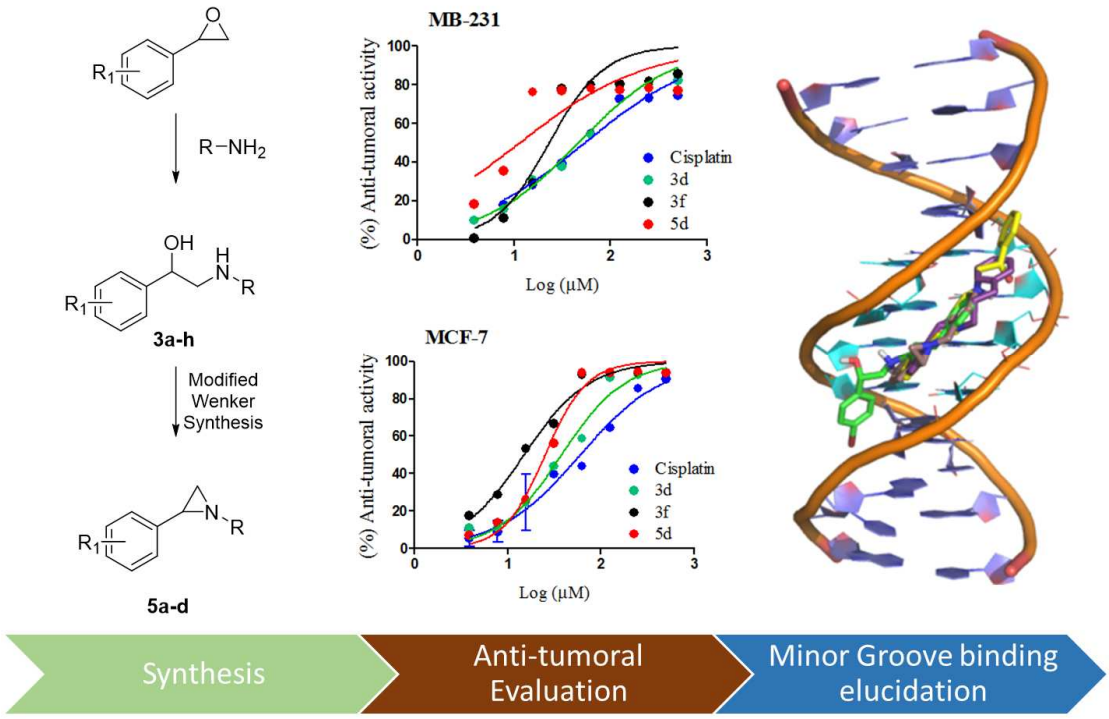

β-amino alcohols and their respective 2-phenyl-N-alkyl aziridines as potential DNA minor groove binders

Miguel M. Vaidergorn[1*], Zumira A.Carneiro[2], , Carla D. Lopes[2], Sérgio de Albuquerque[2],Felipe C.C Reis[3], , Sofia NIkolaou[3], Juliana F.R. Mello[4], Giovani L.Genesi[4], Gustavo H. G. Trossini[4], A. Ganesan[5], Flavio S. Emery[1*]

[1] Departament of Pharmaceutical Sciences, School of Pharmaceutical Sciences of Ribeirão Preto – FCFRP-USP. University of São Paulo, Avenida do Café s/n, 14040-903, Ribeirão Preto, SP, Brazil.

[2] Department of Clinical Analyses, Toxicology and Food Science, School of Pharmaceutical Sciences of Ribeirão Preto – FCFRP-USP. University of São Paulo

[3]Departament of Chemistry, Faculty of Philosophy, Sciences and letters at Ribeirão Preto – FFCLRP-USP

[4] LITEC, Departament of Pharmacy, School of Pharmaceutical Sciences – University of São Paulo, Avenida Prof. Lineu Prestes, 580, bloco 13 superior. São Paulo, SP, Brasil, 05508-000

[5]School of Pharmacy, University of East Anglia, Norwich, UK

* flavioemery@usp.br

KEYWORDS: Aziridines, Triple Negative Breast Cancer, minor groove binding, β-amino alcohols

ABSTRACT: It is known that aziridines and nitrogen mustards exert their biological activities, especially in chemotherapy, via DNA alkylation. The studied scaffold, 2-phenyl-1-aziridine, provides a distinct conformation compared to commonly used aziridines, and therefore, leads to a change in high-strained ring reactivity towards biological nucleophiles, such as DNA. The above series of compounds was tested in three breast cell lines: MCF-10, a healthy cell; MCF-7, a hormone responsive cancer cell; and MDA-MB-231, a triple negative breast cancer cell. Both aziridines and their precursors, β-amino alcohols, showed activity towards these cells, and some of the compounds showed higher selectivity index than cisplatin, the drug used as control. When the type of cell death was investigated, the synthesized compounds demonstrated higher apoptosis and lower necrosis rates than cisplatin, and when the mechanism of action was studied, the compounds were shown to interact with DNA via its minor groove instead of alkylation or intercalation.

1.Introduction

Targeting DNA and drug-DNA interactions has been of great importance since the second half of the 20th century.[1] Small molecules can interfere with the DNA functions either by modulating transcription or by interfering with cell growth and replication as inhibitors.[2] Although they have been studied for decades, the mechanisms of DNA-drug interactions are still not fully comprehended.

There are two main modes of drug-DNA binding.[3] The covalent type found in alkylating agents may act via three mechanisms:[4] irreversible covalent binding with guanine (such as cisplatin and aziridines); cross-link formation between atoms of DNA (two bases are linked by an alkylating agent that has two binding sites, such as nitrogen mustards); and nucleotide mispairing, resulting in a mutation by covalent interaction, and consequently leading to apoptosis;[5] The non-covalent binding involves intercalation and minor groove binders. The first one is found in planar organic compounds and act by π-π stacking between DNA base pairs and the aromatic portion of the molecule. This leads to structural changes in the DNA itself, because intercalation can unwind the DNA double helix. [4]

Minor groove binders are small molecules, usually in a crescent-like shape (Figure 1), that interact by Van der Waals interactions and hydrogen bonds in the minor groove of the DNA double strand.[1, 3, 6] They typically have several heterocyclic aromatic rings and

are commonly employed to bind to specific adenine-thymine (AT)-rich sequences. Netropsin, a polyamide with antibiotic and viral properties, and pyrrole-imidazole polyamides are examples of DNA-binding agents.

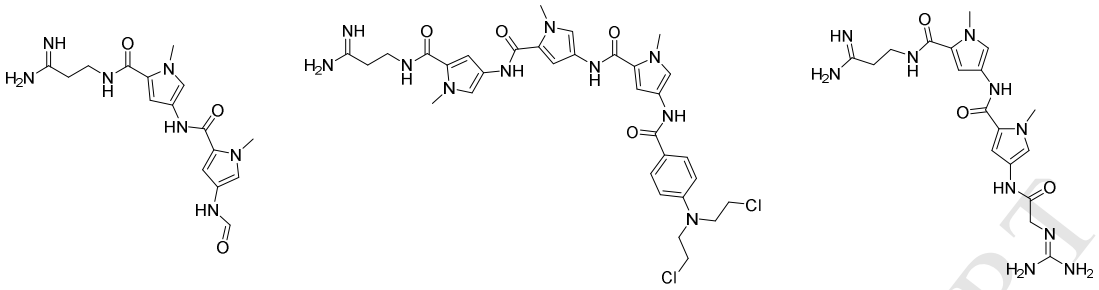

Distamycin A Tallimustine Netropsin

Figure 1. Crescent-like shape molecules used as minor groove binders

Minor groove binders are also used in chemotherapy in several types of cancer, such as carcinoma and ovary and breast cancer (BRCA).[7] Among them, the latter is the most prevalent type of cancer in women worldwide, representing 12% of all new cases of cancer and 25–30% of all cancers in women.[8, 9] According to the American Cancer Society, in the USA alone, approximately 266,120 (30% of all) new cases of invasive breast cancer will be diagnosed in women and more than 41,400 (14%) women are estimated to die in 2018 from it.[10] BRCA is a heterogenous disease in which multiple subtypes are identified—each one showing distinctive profiles of prognosis, physiopathology, and treatments.

Several BRCA subtypes present well established therapy guidelines such as the use of hormonal adjuvant treatment in hormone-sensitive cancers to block estrogen effects for estrogen- (ER) and progesterone-positive (PR) cancers.[10] When the subtype is PR and ER negative but HER2 positive, monoclonal antibodies and tyrosine kinase inhibitors (such as trastuzumab and lapatinib, respectively) are effective.[11, 12] When immunohistochemical analysis shows no hormone receptors on breast cancer cell and the cell is HER2 negative, it is called triple negative breast cancer (TNBC). TNBC accounts for 15–20% of all cases. [13] Although TNBC is primarily treated with chemotherapy, the lack of specific molecular targets leads to low efficacy, consequently leading to a difficult, more aggressive, and less effective treatment. TNBC usually leads to poor prognosis and a high propensity for metastasis progression and chemotherapy resistance.[13] Since there are no targeted therapies specifically for this type of cancer, cytotoxic chemotherapy remains the best option to date.[14] Alkylating-like agents such as platinum derivatives associated with doxorubicin and bevacizumab are used for the treatment of TNBC.[15-17]

In this work, as part of our continuous efforts to find cytotoxic antitumor candidates, we herein report the discovery of aziridine and β-amino alcohol minor-groove binders possessing cytotoxicity against TBNC cells. First, we synthetized both β-amino alcohols and their correspondent azidirines and evaluated their biological activity towards healthy and cancer cell lines. Then, since the compounds presented activity and selectivity, we studied the mechanism of action by flow cytometry and drug-DNA interactions, which demonstrated a non-conventional mechanism of action. Finally, we compared these results to molecular docking, which corroborated the experimental results.

2. Results and discussion

2.1 Chemistry

. The synthesis of 2-phenyl-1-aziridine series **5a-d** involved intramolecular cyclization of the corresponding β-amino alcohol **3**, which was prepared by aminolysis of the epoxide starting

material, via a modified Wenker synthesis[18-20] (Scheme 1). This strategy facilitated the development of a homologue series of N-substituted side chain to study the influence of the length of alkyl chain between each of the aromatic portions in both amino alcohols and aziridines towards the presented biological activity.

Initially, amino alcohols **3a-h** were obtained by ring-opening of styrene oxides (**1a** and **1b**) using several amines (**2a-g**) in a solvent-free methodology. Since aminolysis is not regiospecific, both the regioisomers were obtained, which were easily separated by crystallization or chromatography. Then, the desired amino alcohol was allowed to react with chlorosulfonic acid or sulfuryl chloride to produce the corresponding sulfonyl esters **4a-d**. Finally, after treatment of sulfonyl esters with a base, aziridines were successfully synthesized in varying yields (35–70% in a 1 mmol scale).

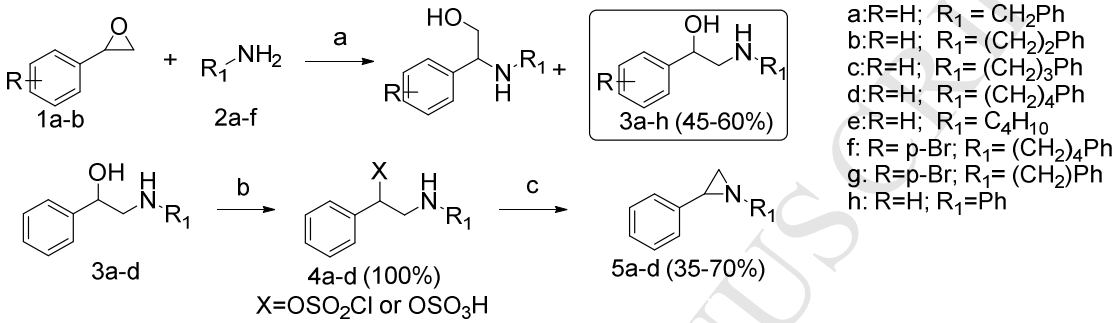

Scheme 1. Synthetic approach for compounds of interest. Conditions: (A) 200℃, 4 h or room temperature (r.t) H_2O, 6 h (when aniline is used); (B) 1, 2 eq. $ClSO_3H$ or SO_2Cl_2, 0℃, Et_2O/DCM; (C) NaOH 6 M/toluene (10:1), 100℃, 18 h

2.2 Biological evaluation

The small library of amino alcohols and respective aziridines were screened against the following targets: i) healthy breast tissue MCF-10; ii) hormone-responsive breast cancer MCF-; and iii) TNBC cell line MB-231. Their half maximal inhibitory concentration (IC_{50}), LD_{50}, and selectivity index (SI) are shown in Table 1. The MTT assays were conducted by following the Mosmann methodology[21]. The cytotoxicity of the studied compounds was compared with cisplatin, which is a drug prescribed for several types of breast cancers and an alkylating-like agent. Based on the results shown in Table 1, some compounds of the two classes studied presented higher selectivity towards cancer cell lines than cisplatin, and higher SI. However, cisplatin showed lower toxicity (higher CC_{50}). It was observed that the longer the alkyl chain between the aromatic rings (from methyl to butyl—as seen in scheme 1), the higher the activity in both amino alcohols and aziridines. Furthermore, a difference in selectivity between β-amino alcohols and their corresponding aziridines was observed. In the MCF7 cell line, β-amino alcohols presented a higher SI, while aziridines showed higher activity and SI towards the MB-231 cell line.

MB-231 cell line was of special interest because of the lack of therapeutic drugs with high SI or efficacy for the long-term treatment of TNBC. The synthetized compounds presented cytotoxic effects, especially the longest alkyl chain β-amino alcohol **3d** and its respective aziridine **5d**, when compared to cisplatin in terms of both IC_{50} (50.76, 11.09, and 78.14 µM, respectively) and SI (2.11, 4.08, and 0.92, respectively). Aziridines **5a**, **5b,** and **5c** also showed higher activity than cisplatin, but with a higher IC_{50} (40.42, 19.00, and 19.8 µM) and lower SI (1.01, 1.97, and 1.77). In addition, **3f** presented a high activity comparable to aziridines, indicating that a minor change in one of the aromatic moieties can lead to an increase in activity. These same compounds presented higher activity than cisplatin against the MCF-7 cell line. However, β-amino alcohols with longer chains presented a higher SI (2.02, 2,88, 4.04, and 2.18 for **3c**, **3d**, **3f** and **3g**, respectively, whereas cisplatin showed a value of 1.45), although they did not necessarily present the best values for IC_{50}.

Table 1: Anti-tumor activity (IC_{50}), cytotoxicity (CC_{50}), and selectivity indices (SI) of the compounds.

Compounds	$IC_{50MCF-7}$ (μM)	IC_{50} MDA-MB231(μM)	CC_{50} MCF-10(μM)	SI_{MCF-7}	$SI_{MDA-MB231}$
3a	209.60 ± 3.10	225.30 ± 3.85	201.60 ± 4.45	0.96	0.89
3b	318.50 ± 0.45	189.90 ± 5.9	197.50 ± 5.40	0.62	1.04
3c	96.40 ± 2.77	101.80 ± 1.79	195.60 ± 0.75	2.02	1.92
3d	37.17 ± 1.34	50.76 ± 2.47	107.30 ± 4.7	2.88	2.11
3e	279.60 ± 1.5	259.40 ± 4.17	187.70 ± 5.76	0.67	0.72
3f	14.48 ± 0.61	22.71 ± 0.21	58.54 ± 1.33	4.04	2.57
3g	53.01 ± 2.66	73.89 ± 3.12	115.60 ± 0.95	2.18	1.56
3h	236.20 ± 5.35	236.90 ± 4.92	316.16 ± 4.85	1.33	1.33
5a	27.83 ± 0.42	40.42 ± 1.34	40.99 ± 0.25	1.47	1.01
5b	169.70 ± 5.99	19.00 ± 0.90	37.57 ± 1.5	0.2	1.97
5c	24.50 ± 1.11	19.89 ± 2.23	35.43 ± 1.31	1.44	1.77
5d	24.72 ± 0.5	11.09 ± 0.39	43.30 ± 0.03	1.83	4.08
Cisplatin	49.26 ± 0.21	78.14 ± 2,4	72.14 ± 4.12	1.45	0.91

2.3 Mechanism of action investigation

Since compounds **3d, 3f,** and **5d** showed high tumorigenic activity, especially against the MB-231 cell line, they were selected for further studies to elucidate the mechanism by which they induced cell death. In a simple approach, the detection of externalization of phosphatidylserine was performed by staining with Annexin V/propidium iodide (PI) (Figure 2A) via flow cytometry. Both **3f**- and **5d**-treated MB-231 cells induced apoptosis above 75% of MB-231 population (**3f** = 91.3% and **5d** = 77%, Figure 2B). The percentage of early apoptotic cells (Annexin V simple stain) was higher in **3f**-treated cells (33.6%; Figure 2C). Notably, **5d** treatment resulted in late apoptosis/necrosis in the cells (Annexin V/PI stained) (Figure 2D). This result was in agreement with MTT results and suggests that **3f** and **5d** are cytotoxic to cancer cells, and they probably induced apoptosis by different mechanisms.

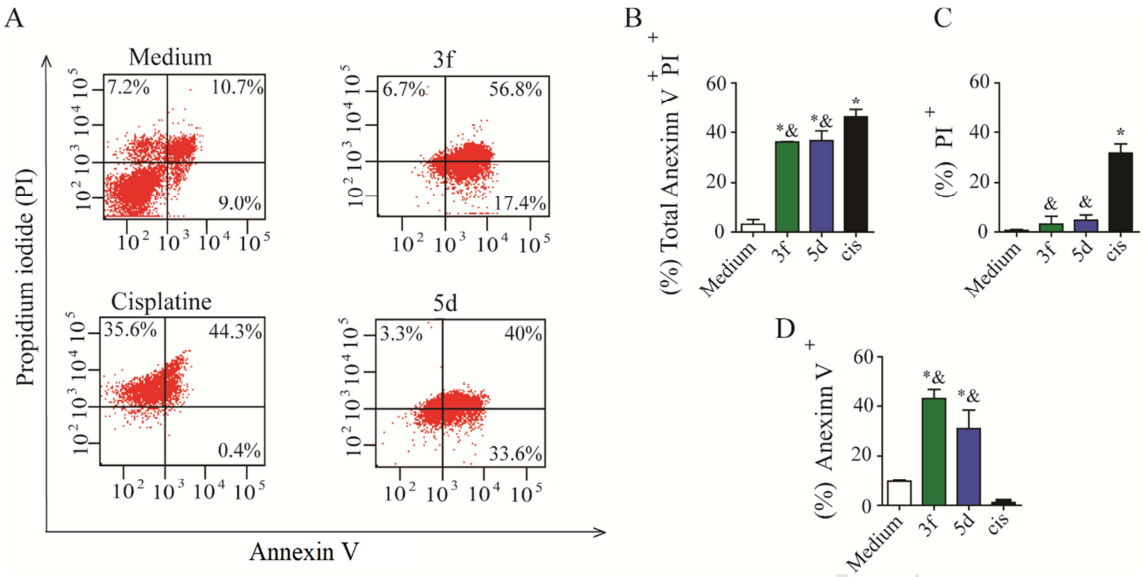

Figure 2. Phenyl aziridines selectively lead to apoptosis of breast tumor cells. Representative dot plot of each compound (A). Treatment with 3f and 5d showed higher tumorigenicity (B). 3f treatment led to early apoptosis (C). 5d and 3f together showed the same ability to lead to late apoptosis/necrosis (D). Results are presented as the mean of triplicate experiments.

Based on the results of flow cytometry assay, we aimed to investigate the mechanism of action of these compounds and why they direct cell death to a different direction when compared to cisplatin. Although it is known that nitrogen mustards and aziridines act as electrophiles for biological nucleophiles such as nitrogenous bases in the DNA, we were not sure whether the same mechanism would apply for the compounds tested in this study because of the electronic and conformational differences between the different types of compounds.

It is well documented in literature that polymethylene analogs of drug candidates can enhance biological activity.[22, 23] This can be caused either by increasing the interaction with active site or by altering the physicochemical properties related to hydrophobicity, such as partition coefficient, solubility in water, and critical micelle concentration. This effect seems to be corroborated by the cancer activity results obtained in the present study. To investigate this result further, we performed an assay to probe the potential interaction between DNA and the studied structures (full experimental details of ct-DNA interaction experiment in the experimental procedure). Based on the results obtained in the cancer cells, two compounds, **3d** and its respective aziridine **5d**, were chosen to study the potential interaction with DNA. These two molecules have the longest alkyl chain between the aromatic moieties tested and the highest activities when there are no substituents in the aromatic ring. **3d** and **5d** were incubated with ct-DNA in buffer solution at 32°C for 5 min before recording each electronic spectrum. The binding constant (K_b) for each compound-DNA adduct was obtained using the Benesi-Hildebrand equation (see supplementary information) to verify the relative strength of interaction of **3d** and **5d** with DNA.

Depending on the type of interaction with DNA, ultraviolet (UV)-visible spectra exhibited distinct profile changes. Compounds that bound through intercalation exhibited hypochromism on the DNA band centered at 260 nm. To intercalate, the compound must have a planar and rigid structure, which is usually provided by the presence of fused aromatic rings. [24-26] In contrast, hyperchromic effect in DNA absorption indicates the changes in the secondary structure of double helix, which in turn exposes the nitrogenous bases to the solvent, thereby increasing the absorption of these

chromophores. This kind of change may arise from covalent, groove, or electrostatic binding.[18] It is rather difficult to distinguish them exclusively based on spectrophotometric titration. However, previous studies have reported that a combination of hyper-and hypsochromism indicates a covalent interaction such as alkylation, while hyperchromism alone is observed when a non-covalent binding takes place.[17-21] As seen in Figure 4, both **3d** and **5d** caused hyperchromism in absorption band of DNA at 260 nm following DNA-compound interaction, without any hypsochromic or bathchromic changes.[4, 25, 27]

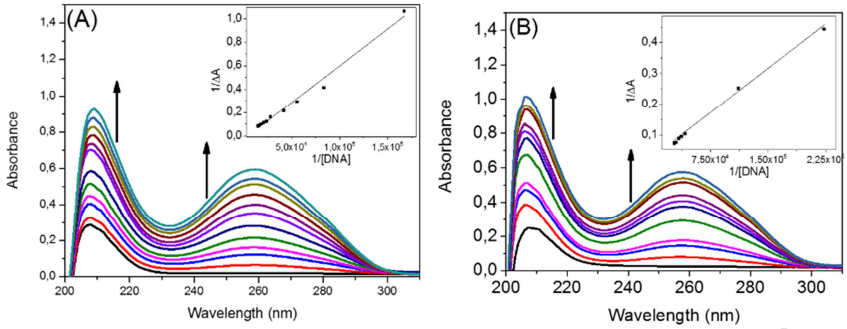

Figure 4. UV-Vis spectra of (A) 3d (10^{-6} mol L^{-1}) and (B) 5d ($1{,}25x10^{-8}$ mol L^{-1}) with increasing concentrations of *ct*-DNA (from $4.9x10^{-5}$ to $4.9x10^{-4}$ mol L^{-1}) in Tris buffer (5 mM tris(hydroxymethyl)aminomethane hydrochloride (Tris), 50 mM NaCl, pH 7.4). Insert: double reciprocal Benesi-Hildebrand plot.

Owing to this observation, it is suggested that minor groove binding is a more favorable type of interaction.[24] This kind of weak interaction is typical for structures bearing unfused aromatic rings, such as phenyl groups of **3d** and **5d,** bound to flexible carbon chains, which have torsional freedom.[20] These features present in the molecules under investigation in this study, leads to accommodation in the minor groove of DNA, which might be directed by hydrophobic interaction, hydrogen bonding, and/or electrostatic interactions. Usually minor groove binding is preferred to major groove binding owing to a closer in-space interaction of the former and steric hindrance of the latter due to the presence of the amine group on C2 of guanine.[20] Presumably, in our case, the interaction of both species are hydrophobic in nature because of their relatively long alkyl chain. In the case of compound **3d**, it is reasonable to assume the assistance of hydrogen bonds, since this compound bears OH and NH groups in its structure. These assumptions are corroborated by the docking results (*vide infra*). Finally, if DNA is assumed to be the target responsible for the observed cytotoxicity, the different kinds of interactions of **3d** and **5d** (groove binding) when compared to cisplatin (alkylation) is probably responsible for triggering different mechanisms of cell death.

The Kb values observed in this study (**3d** Kb = 1,592 x 10^5, and **5d** Kb = 5,233 x 10^5) are consistent with data reported earlier from similar spectrophotometric titration, suggesting a strong interaction between **3d** and **5d** with ct-DNA.[25] To confirm the binding mode in DNA, molecular docking was performed for the most active derivatives. Autodock 4.2 software was used for calculations, and the Lamarckian Genetic Algorithm was selected as a search method.[28] Ligands were constructed using Spartan 10 WAVEFUNCTION, and Merck Molecular Force Field (MMFF) was applied for conformer distribution. The charges were calculated using PM6 following the density functional theory (DFT) method.

2.4 Molecular docking validation

Molecular docking validation was performed in two steps. First step 1 (VS 1) was performed using re-docking of netropsin in all DNA structures, checking whether the

selected parameters were able to identify the correct region of interaction. Netropsin was selected for docking validation as it is a well-known minor groove ligand. In validation step 2 (VS 2), a reduced grid box was applied to perform a more accurate assessment of interactions with the DNA region.

The parameters used in docking validation, which considered all DNA, were able to produce most of the conformational states of netropsin bound in the minor groove, as expected. The binding region at the minor groove was rich in A-T base pairs and was in accordance with the known binding mode. After identification of the binding region, calculations were focused in the minor groove region. The best conformer presented a predicted binding energy of -7.74 kcal/mol. This binding mode was similar to the binding mode obtained by Ricci et al. for netropsin docking[29].

The best parameter set was applied in the molecular docking of Hoechst-33258 (minor groove binder), **3d**, **3f**, **5a**, and **5c** derivatives.

An additional evaluation of the method was executed using Hoechst-33258, a DNA inhibitor that binds at the minor groove region. [30] Results showed that parameters of both VS 1 and VS 2 were able to identify the correct region of binding as well as the correct AT-rich region of binding. Molecular re-docking focusing on minor groove returned the conformer with a predicted binding energy of -4.80 kcal/mol (SM).

The molecular docking of **3f** was performed using both methods, and the results showed that the minor groove was the preferred region of binding, which was in accordance with the experimental assays (Figure 4). This amino alcohol derivative (**3f**) showed interactions with AT-rich region, and the best conformer exhibited a predicted binding energy of -8.51 kcal/mol. The proximity of the aromatic ring of the ligand and DNA backbone suggests interactions between these groups (Figure 5). **3f** is also involved in one hydrogen bond with the backbone at regions DA19 and DT18, besides a hydrogen bond with thymine of the DT18 base pair (Figure 5b). Although this interaction profile was not very common for inhibitors that interact with the minor groove, the role of ligand-DNA backbone interactions could be important for elucidating the mechanism of action. Interactions between ligands and the sugar atoms of DNA backbone could promote stabilization of the complex[31].

The proximity of the aromatic ring of the ligand and the sugar atoms of DNA backbone is not exclusive to **3f** derivative. Other derivatives also showed this profile, suggesting interactions between these atoms of the DNA. The best conformer of this derivative showed a predicted binding energy of -8.42 kcal/mol. The derivatives **5a** and **5c** interact mainly through hydrophobic interactions with DNA (Figure 5c-d). Consequently, their predicted energies of binding were poorer than **3d** and **3f** derivatives. The predicted binding energies for **5a** and **5c** were -3.96 and 5.36 kcal/mol, respectively. **3d** derivative showed two hydrogen bonds with the DNA backbone at DT6 and DA7 regions, besides one hydrogen bond with thymine of the DT6 base pair (Figure 5e). These results corroborated the experimental tests and provided a new insight of how β-amino alcohols and aziridines can interact with DNA and the importance of an aromatic moiety in the scaffold.

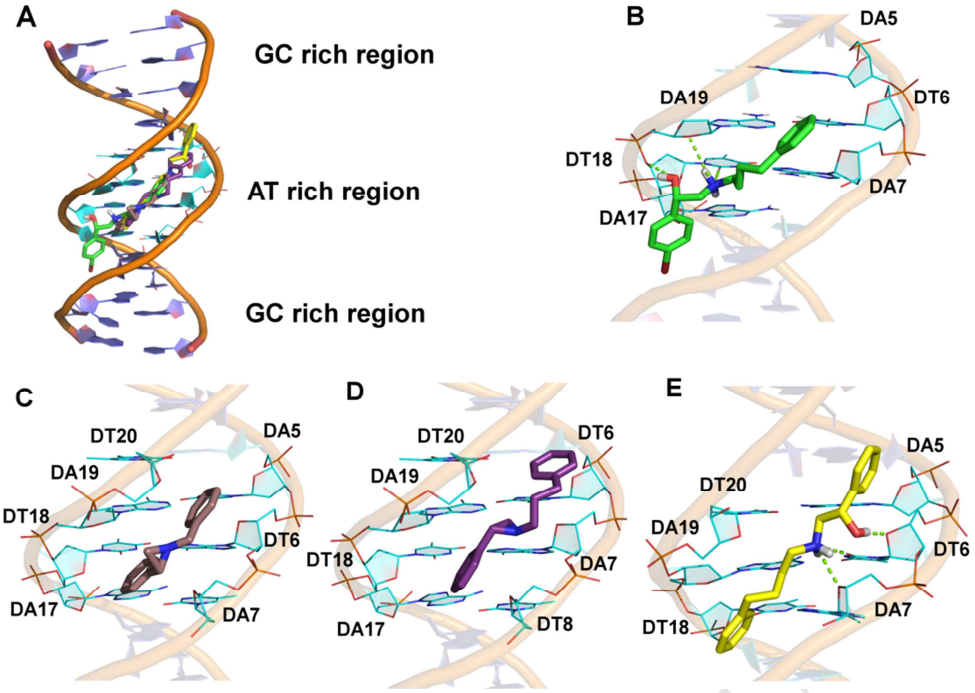

Figure 5. Molecular docking showing minor groove binding in AT-rich regions (A) of derivatives 3f (B), 5a (C), 5c (D) and 3d (E).

3. Conclusion

In conclusion, we synthesized amino alcohols **3a-h** and 2-phenyl-1-aziridine series **5a-d** and biologically evaluated these compounds. The results of this study provide new insights into the mechanism of action of β-amino alcohols and 2-phenyl-N-alkyl aziridines and their interaction with DNA, especially in two breast cancer cell lines. The mechanism of action was found to be spatial conformation, leading to a crescent-like shaped molecule, although they are small molecules. Moreover, the new compounds were more selective than cisplatin in both the cell lines and may provide evidence for further studies on new therapies for TNBC.

Author contributions

The manuscript was written through contributions of all authors. All authors have given approval to the final version of the manuscript.

Acknowledgment

The authors thank 'Fundação de Amparo à Pesquisa de São Paulo" (processes 2014/03812-9 and 2015/20302-7) for providing financial support during this research.

4. Experimental session

4.1 Chemistry

4.1.1 General information

^{1}H and ^{13}C NMR NMR spectra were determined on a BRUKER® Fourier300 – Ultra Shield® spectrometer in $CDCl_3$ or DMSO-d_6. The reagents were all analytical grade or chemically pure acquired from Sigma-Aldrich. Flash chromatography was performed on silica gel (60Å, 230-400mesh, 40-63µm).

4.1.2 General procedure for synthesis of the β-aminoalcohols

Epoxide (1a-b, 2 mmol, 1 eq) was slowly added during 1 hour to the amine (4mmol, 2eq) in a round-bottom flask in reflux. After the addition was completed, the reaction mixture was stirred at the amine boiling point for 3h and then cooled to room temperature. The oily product solidified over time and was recrystallized in dichlorometane-hexane (2:8). When necessary, an additional purification was carried out in a short flash chromatography column (Ethyl Acetate-Methanol).

2-(benzilamine)-1-phenylethan-1-ol (3a)
White crystals, 55% yield. ^{1}H RMN (300 MHz, MeOD) δ 7,39 – 7,16 (m, 10H), 4,77 (dd, J = 8,5, 4,5 Hz, 1H), 3,78 (dt, J = 22,2, 7,7 Hz, 1H), 2,86 – 2,65 (m, 2H).^{13}C NMR (75 MHz, MeOD) δ 144,60; 140,5; 129,5; 129,4; 128,5; 128,3; 127,0; 73,4; 57,4; 54,2.

2-(phenetilamine)-1-phenyletan-1-ol (3b)
White crystals, 54% yield. ^{1}H RMN (300 MHz, CDCl3) δ 7,34 – 7,10 (m, 10H), 4,74 (dd, J = 9.4, 3.4 Hz, 1H), 2,92 – 2,84 (m, 2H), 2,83 – 2,76 (m, 2H), 2,75 – 2,67 (m, 2H). ^{13}C NMR (75 MHz, CDCl3) δ 142,1; 142,0; 139,1; 128,8; 128,6; 128,5; 127,7; 126,5; 125,8; 71,2; 56,6; 50,5; 35,7.

1-phenyl-2-((3-phenylpropyl)amino)ethan-1-ol (3c)
White crystals,42% yield. ^{1}H RMN (300 MHz, CDCl3) δ 7,42 – 7,00 (m, 10H), 4,66 (dd, J = 8,5; 4,5 Hz, 1H), 2,65 (t, J = 6.,7 Hz, 2H), 2,62 – 2,50 (m, 4H), 1,73 (dt, J = 15,1; 7,5 Hz, 2H). ^{13}C NMR (75 MHz, CDCl3) δ 147,1; 145,6; 131,9; 131,9; 131,1; 129,5; 129,4; 75,8; 60,6; 37,0; 34,8

1-phenyl-2-((4-phenylbutyl)amino)ethan-1-ol (3d)
Yellow solid, 45% yield. ^{1}H RMN (300 MHz, MeOD) δ 7,44 – 6,89 (m, 10H), 4,68 (dd, J = 7,8; 5,3 Hz, 1H), 2,69 (dd, J = 7,9; 4,8 Hz, 2H), 2,57 (ddd, J = 14,7; 10,0; 5,2 Hz, 4H), 1,64 – 1,41 (m, 4H). ^{13}C NMR (75 MHz, CDCl3) δ 142,2; 128,5; 128,5; 128,4; 127,7; 125,9; 77,1; 71,1; 56,7; 49,1; 35,7; 29,0; 28,8.

2-(butylamino)-1-phenylethan-1-ol (3e)
Yellow solid, 42% yield.^{1}H RMN (300 MHz, CDCl3) δ 7,36 – 7,12 (m, 5H), 4,92 (dd, J = 9,8; 2,9 Hz, 1H), 2,88 (ddd, J = 5,96; 11,3; 4,8 Hz, 2H), 2,72 (tdd, J = 11,9; 7,8; 4,3 Hz, 2H), 1,28 (dt, J = 15,0; 7,4 Hz, 4H), 0,76 (t, J = 7,4 Hz, 3H) ^{13}C NMR (75 MHz, CDCl3) δ 141,7; 128,8; 127,7; 125,8; 70,5; 65,9; 48,8; 31,4; 20,3; 13,8.

1-(4-bromophenyl)-2-((4-phenylbutyl)amino)ethan-1-ol (3f)
Yellowish solid, 15% yield. ^{1}H RMN (300 MHz, CDCl3) δ 7,64 – 6,97 (m, 14H), 5,08 (dd, J = 10,0; 2,5 Hz, 1H), 3,07 – 2,97 (m, 1H), 2,95 – 2,77 (m, 3H), 2,63 (dt, J = 15,0; 5,6 Hz, 3H), 1,84 – 1,60 (m, 5H). ^{13}C NMR (75 MHz, CDCl3) δ 141,6; 140,0; 131,7; 128,4; 128,3; 127,5; 126,0; 121,9; 69,4; 55,7; 48,7; 35,4; 28,6; 27,1.

2-(benzylamino)-1-(4-bromophenyl)ethan-1-ol (3g)
Yellow solid, 10% yield. ^{1}H RMN (300 MHz, DMSO) δ 7,50 – 7,27 (m, 9H), 4,65 (t, J = 6,1 Hz, 1H), 3,73 (d, J = 2,7 Hz, 2H), 2,61 (d, J = 6,2 Hz, 2H). ^{13}C NMR (75 MHz, DMSO) δ 143.9, 140.3, 130.7, 128.1, 128.1, 127.9, 126.6, 119.7, 70.7, 56.5, 52.5.

1-phenyl-2-(phenylamino)ethan-1-ol (3h)
Orange oil, 70% yield. ^{1}H RMN (300 MHz, CDCl3) δ 7,49 – 6,50 (m, 10H), 4,53 (dd, J = 6,9; 4,2 Hz, 1H), 3,95 (dd, J = 11,1; 4,2 Hz, 1H), 3,76 (dd, J = 11,1; 7,0 Hz, 1H). ^{13}C NMR (75 MHz, CDCl3) δ 146.1, 139.4, 129.1, 128.8, 128.6, 127.7, 126.9, 118.7, 114.7, 77.4, 77.0, 76.6, 66.9, 60.8.

4.1.3 – General procedure for the synthesis of aziridines

To a solution of **3** (1mmol) in ethyl ether/dichlorometane (8:2) at 0℃, chlorossulfonic acid or sulfonyl chloride was slowly added (1.2mmol). After stirring at 0℃ for 1h, the reaction mixture was stirred at room temperature for 2h30. The resulting white solid was washed and filtered using 0℃ ethyl ether (3x10 ml), isopropyl alcohol (3x10ml) and ethyl ether (3x10ml) and was dried under low pressure, resulting in **4**(a-d) in quantitative yields. To a solution of **4** (a-d - 1mmol) in toluene (5ml), NaOH of 6,2M (4,96g in 20ml) was added and the reaction was refluxed for 18h. The reaction mixture was then extracted with ethyl acetate (3x20ml), dried over Na_2SO_4 and the solvent was evaporated. The resulting oil was purified over deactivated silica gel (1% Et_3N) in hexane: ethyl acetate. The purified compounds were kept under refrigeration and covered from light.

1-benzyl-2-phenylaziridine (5a)
Incolor oil, 55% yield. ^{1}H RMN (300 MHz, CDCl3) δ 7,50 – 7,15 (m, 10H), 3,72 (d, J = 13,7 Hz, 1H), 3,63 (d, J = 13,8 Hz, 1H), 2,53 (dd, J = 6,5; 3,4 Hz, 1H), 2,01 (d, J = 3,3 Hz, 1H), 1,88 (d, J = 6,5 Hz, 1H). ^{13}C NMR (75 MHz, CDCl3) δ 140.1, 139.1, 128.3, 128.3, 127.8, 126.9, 126.9, 126.2, 64.7, 41.5, 37.9.

1-phenethyl-2-phenylaziridine (5b)
Incolor oil, 60% yield. ^{1}H RMN (300 MHz, CDCl3) δ 7,46 – 7,12 (m, 10H), 2,94 (t, J = 7,6 Hz, 2H), 2,68 (m, J = 11,4; 7,4 Hz, 2H), 2,30 (dd, J = 6,5; 3,4 Hz, 1H), 1,92 (d, J = 3,4 Hz, 1H), 1,67 (d, J = 6,6Hz, 2H). ^{13}C NMR (75 MHz, CDCl3) δ 140,2; 140,0; 128,8; 128,3; 128,2; 127,1; 126,1; 126,0; 63,3; 41,4; 37,9; 36,4.

2-phenyl-1-(3-phenylpropyl)aziridine (5c)
Incolor oil, 50% yield. ^{1}H RMN (500 MHz, CDCl3) (300 MHz, CDCl3) δ 7,36 – 7,13 (m, 10H), 2,76 – 2,70 (m, 2H), 2,54 (dt, J = 11,6; 7,2 Hz, 1H), 2,44 – 2,33 (m, 1H), 2,31 (dd, J = 6,5; 3,3 Hz, 1H), 1,98 (dd, J = 15,5; 7,1 Hz, 2H), 1,91 (d, J = 3,4 Hz, 1H), 1,67 (d, J = 6,5 Hz, 1H).). ^{13}C NMR (75 MHz, CDCl3) δ 142,2; 140,4; 128,5; 128,4; 128,4; 126,9; 126,2; 125,8; 61,1; 41,4; 37,8; 33,7, 31,4.

2-phenyl-1-(4-phenylbutyl)aziridine (5d)
Incolor oil, 65% yield.^{1}H RMN (300 MHz, CDCl3) (300 MHz, CDCl3) δ 7,49 – 6,82 (m, 10H), 2,65 (t, J = 7,3 Hz, 2H), 2,51 (dt, J = 11,7; 6,8 Hz, 1H), 2,44 – 2,35 (m, 1H), 2,31 (dd, J = 6,5; 3,3 Hz, 1H), 1,90 (d, J = 3,2 Hz, 1H), 1,81 – 1,70 (m, 4H), 1,67 (d, J = 6,6

Hz, 2H). ^{13}C NMR (75 MHz, CDCl3) δ 142,4; 140,4; 128,4; 128,2; 126,8; 126,2; 125,6; 61,6; 41,2; 37,8; 35,8; 29,4; 29.2.

4.2 MTT assay

The cytotoxity was assessed using the classical [3 – (4,5-dimethylthiazol-2-yl) -2,5-diphenyl tetrazolium bromide] (MTT) colorimetric assay[16]. To this end, 5.0 x 10^5 cells (MCF-10, MCF-7 and MDA-MB231) were incubated for 24 hours in 96-well cell culture. After this incubation period, the compounds or cisplatine was added (concentrations 500 to 3.9 µM in serial dilution / compounds solubilized in DMSO 0,5%) in a final volume of 200 µL. Cells were incubated for 48 hours at 37 ℃. Aft er incubation with the compounds, the medium was removed and added 50 µL of MTT (2.0 mg/mL) diluted in phosphate buffered saline (PBS). The precipitated blue MTT formazan was then dissolved in 50 µL of DMSO, and the absorbance was measured at 570 nm in a VARIAN CARY-50 plate reader MPR multiwell. Cell viability was expressed as the percentage of absorption values in treated cells compared with untreated (control) cells. IC_{50} curve fitting was carried out using GraphPad Prism 5 Software (GraphPad Software Inc., San Diego, CA).

4.3 Flow cytometry assay

To evaluate the apoptosis events, MDA-MB-231 cells were seeded in 12-well plates at 5.0 x 10^6 cells/well for 24 h. Next, they were treated with 3f and 5d compounds or cisplatin as positive control for 48 h. After, the cells were trypsinized, washed with ice-cold PBS and re-suspended in binding buffer, according to the kit instructions. The cells were then incubated with FITC-conjugated Annexin V (1:100) for another 15 min as recommended by FITC Annexin V Apoptosis Detection Kit (BD Pharmigen ™). Propidium iodide (1 µg/mL) was added immediately before BD FAXCANTO™ flow cytometer analysis. The excitation/emission used for FITC- conjugated Annexin V was 494/518 nm while to propidium iodide, the excitation/emission was 585/617 nm. A total of 10,000 events were counted per sample and analyzed by the software BD FACSDIVA (BD Biosciences).

4.4 DNA samples and binding experiments

Calf-thymus deoxyribonucleic acid (ct-DNA) was obtained from Sigma-Aldrich. It was used as received and stored below 277 K. Ct-DNA was dissolved in a buffer solution (5 mM tris(hydroxymethyl)aminomethane trishydrochloride (Tris), 50 mM NaCl, pH 7.4) and stirred for about 12 hours. The resulting solution of ct-DNA gave ratios of UV absorbance at 260 and 280 nm, A_{260}/A_{280}, in between 1.8-1.91, suggesting that the ct-DNA was sufficiently free of proteins. In this case, the ratio of A_{260}/A_{280} was 1.86. The concentration of nucleic acid solutions was determined spectrophotometrically, using □ = 6600 M^{-1} cm^{-1} at 260 nm and it was expressed in terms of base-pair equivalents per dm^3.

First, using a fixed complex concentration (3d = 2.00 µM; 5d = 1.25 µM) it was added aliquots of DNA solution ([DNA] = 3.00 mM) to the sample. The experiment was performed using an UV/Visible Spectrophotometer - UV380G – Gehakain, at 305 K and the complex-DNA solutions were allowed to incubate for 5 minutes before each spectra

recording. The intrinsic binding constants (K_b) of the interaction between compounds and DNA can be calculated using the Benesi-Hildelbrand equation:

$$\frac{[A_0]}{(A - A_0)} = \frac{\varepsilon_C}{(\varepsilon_{D-C} - \varepsilon_C)} x \frac{1}{K_b[DNA]}$$

where, A_0 e A are the absorbances of the drug and the durg-DNA adduct, respectively. ε_C and ε_{D-C} are the absorption coefficients of the drug and the drug–DNA adduct, respectively. K_b is the binding constant and it is obtained from intercept-to-slope ratios of a $1/(A - A_0)$ *versus* 1/[DNA] plots.

4.5 Docking validation

Step 1 (VS 1): The grid box dimensions were 96x96x96 points, considering all DNA structure. Molecular docking genetic algorithm parameters changed from default were population size of 50, number of evaluation of 50000000, for 25 docking runs.

Step 2 (VS 2): In these calculations, the re-docking of neutropsin was performed in a reduced grid box with dimensions of 60x70x50 points, focusing in the region of binding. The parameters changed of the default were population size of 50, number of evaluations of 25000000 and 25 docking runs.

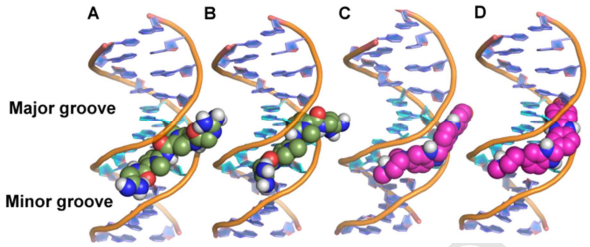

Figure 6. Molecular docking validation using re-docking of neutropsin (green), VS 1 (A) and VS 2 (B). Molecular docking between Hoechst-33258 (pink) and DNA using parameters of VS 1 (C) and VS 2 (D). A-T rich region in blue and G-C rich region in purple.

References

1. Singh, R. K.; Kumar, S.; Prasad, D. N.; Bhardwaj, T. R., Therapeutic journery of nitrogen mustard as alkylating anticancer agents: Historic to future perspectives. *European Journal of Medicinal Chemistry* **2018,** *151*, 401-433.
2. Bailon-Moscoso, N.; Romero-Benavides, J. C.; Ostrosky-Wegman, P., Development of anticancer drugs based on the hallmarks of tumor cells. *Tumor Biology* **2014,** *35* (5), 3981-3995.
3. Puyo, S.; Montaudon, D.; Pourquier, P., From old alkylating agents to new minor groove binders. *Critical Reviews in Oncology Hematology* **2014,** *89* (1), 43-61.
4. Sirajuddin, M.; Ali, S.; Badshah, A., Drug-DNA interactions and their study by UV-Visible, fluorescence spectroscopies and cyclic voltametry. *Journal of Photochemistry and Photobiology B-Biology* **2013,** *124*, 1-19.
5. Polavarapu, A.; Stillabower, J. A.; Stubblefield, S. G. W.; Taylor, W. M.; Baik, M. H., The Mechanism of Guanine Alkylation by Nitrogen Mustards: A Computational Study. *Journal of Organic Chemistry* **2012,** *77* (14), 5914-5921.
6. Moravek, Z.; Neidle, S.; Schneider, B., Protein and drug interactions in the minor groove of DNA. *Nucleic Acids Research* **2002,** *30* (5), 1182-1191.

7. Colvin M. Alkylating Agents. In: Kufe DW, P. R., Weichselbaum RR, et al., editors. Holland-Frei Cancer Medicine. 6th edition. Hamilton (ON): BC Decker; https://www.ncbi.nlm.nih.gov/books/NBK12772/, A. f.
8. Ferlay, J.; Soerjomataram, I.; Dikshit, R.; Eser, S.; Mathers, C.; Rebelo, M.; Parkin, D. M.; Forman, D.; Bray, F., Cancer incidence and mortality worldwide: Sources, methods and major patterns in GLOBOCAN 2012. *International Journal of Cancer* **2015,** *136* (5), E359-E386.
9. Siegel, R. L.; Miller, K. D.; Jemal, A., Cancer Statistics, 2017. *Ca-a Cancer Journal for Clinicians* **2017,** *67* (1), 7-30.
10. Siegel, R. L.; Miller, K. D.; Jemal, A., Cancer Statistics, 2018. *Ca-a Cancer Journal for Clinicians* **2018,** *68* (1), 7-30.
11. Balduzzi, S.; Mantarro, S.; Guarneri, V.; Tagliabue, L.; Pistotti, V.; Moja, L.; D'Amico, R., Trastuzumab-containing regimens for metastatic breast cancer. *Cochrane Database of Systematic Reviews* **2014,** (6).
12. Medina, P. J.; Goodin, S., Lapatinib: A dual inhibitor of human epidermal growth factor receptor tyrosine kinases. *Clinical Therapeutics* **2008,** *30* (8), 1426-1447.
13. Yao, H.; He, G.; Yan, S.; Chen, C.; Song, L.; Rosol, T. J.; Deng, X., Triple-negative breast cancer: is there a treatment on the horizon? *Oncotarget* **2017,** *8* (1), 1913-1924.
14. Isakoff, S. J., Triple-Negative Breast Cancer Role of Specific Chemotherapy Agents. *Cancer Journal* **2010,** *16* (1), 53-61.
15. Anders, C. K.; Carey, L. A., Biology, Metastatic Patterns, and Treatment of Patients with Triple-Negative Breast Cancer. *Clinical Breast Cancer* **2009,** *9*, S73-S81.
16. von Minckwitz, G.; Martin, M., Neoadjuvant treatments for triple-negative breast cancer (TNBC). *Annals of Oncology* **2012,** *23*, 35-39.
17. Sharma, P.; López-Tarruella, S.; García-Saenz, J. A.; Ward, C.; Connor, C.; Gómez, H. L.; Prat, A.; Moreno, F.; Jerez-Gilarranz, Y.; Barnadas, A.; Picornell, A.; del Monte-Millán, M.; Gonzalez-Rivera, M.; Massarrah, T.; Pelaez-Lorenzo, B.; Palomero, M. I.; González del Val, R.; Cortes, J.; Fuentes Rivera, H.; Bretel Morales, D.; Márquez-Rodas, I.; Perou, C. M.; Wagner, J.; Mammen, J. M. V.; McGinness, M.; Klemp, J. R.; Amin, A.; Fabian, C. J.; Heldstab, J.; Godwin, A. K.; Jensen, R. A.; Kimler, B. F.; Khan, Q. J.; Martin, M., Efficacy of neoadjuvant carboplatin plus docetaxel in triple negative breast cancer: Combined analysis of two cohorts. *American Association for Cancer Research* **2016**.
18. Li, X.; Chen, N.; Xu, J., An Improved and Mild Wenker Synthesis of Aziridines. *Synthesis-Stuttgart* **2010,** (20), 3423-3428.
19. Buckley, B. R.; Patel, A. P.; Wijayantha, K. G. U., Observations on the Modified Wenker Synthesis of Aziridines and the Development of a Biphasic System. *Journal of Organic Chemistry* **2013,** *78* (3), 1289-1292.
20. Wenker, H., The preparation of ethylene imme from monoethanolamine. *Journal of the American Chemical Society* **1935,** *57*, 2328-2328.
21. Mosmann, T., RAPID COLORIMETRIC ASSAY FOR CELLULAR GROWTH AND SURVIVAL - APPLICATION TO PROLIFERATION AND CYTO-TOXICITY ASSAYS. *Journal of Immunological Methods* **1983,** *65* (1-2), 55-63.
22. Lui, V. W. Y.; Wentzel, A. L.; Xiao, D.; Lew, K. L.; Singh, S. V.; Grandis, J. R., Requirement of a carbon spacer in benzyl isothiocyanate-mediated cytotoxicity and MAPK activation in head and neck squamous cell carcinoma. *Carcinogenesis* **2003,** *24* (10), 1705-1712.
23. Morse, M. A.; Eklind, K. I.; Amin, S. G.; Hecht, S. S.; Chung, F. L., EFFECTS OF ALKYL CHAIN-LENGTH ON THE INHIBITION OF NNK-INDUCED LUNG NEOPLASIA IN A/J MICE BY ARYLALKYL ISOTHIOCYANATES. *Carcinogenesis* **1989,** *10* (9), 1757-1759.
24. Paul, A.; Bhattacharya, S., Chemistry and biology of DNA-binding small molecules. *Current Science* **2012,** *102* (2), 212-231.

25. Barone, G.; Terenzi, A.; Lauria, A.; Almerico, A. M.; Leal, J. M.; Busto, N.; Garcia, B., DNA-binding of nickel(II), copper(II) and zinc(II) complexes: Structure-affinity relationships. *Coordination Chemistry Reviews* **2013,** *257* (19-20), 2848-2862.
26. Tuite, E.; Sehlstedt, U.; Hagmar, P.; Norden, B.; Takahashi, M., Effects of minor and major groove-binding drugs and intercalators on the DNA association of minor groove-binding proteins RecA and deoxyribonuclease I detected by flow linear dichroism. *European Journal of Biochemistry* **1997,** *243* (1-2), 482-492.
27. Sun, J.; Wu, S.; Chen, H. Y.; Gao, F.; Liu, J.; Ji, L. N.; Mao, Z. W., Synthesis, characterization and DNA-binding and DNA-photocleavage studies of two Ru(II) complexes containing two main ligands and one ancillary ligand. *Polyhedron* **2011,** *30* (12), 1953-1959.
28. Morris, G. M.; Huey, R.; Lindstrom, W.; Sanner, M. F.; Belew, R. K.; Goodsell, D. S.; Olson, A. J., AutoDock4 and AutoDockTools4: Automated Docking with Selective Receptor Flexibility. *Journal of Computational Chemistry* **2009,** *30* (16), 2785-2791.
29. Ricci, C. G.; Netz, P. A., Docking Studies on DNA-Ligand Interactions: Building and Application of a Protocol To Identify the Binding Mode. *Journal of Chemical Information and Modeling* **2009,** *49* (8), 1925-1935.
30. Suntharalingam, K.; Mendoza, O.; Duarte, A. A.; Mann, D. J.; Vilar, R., A platinum complex that binds non-covalently to DNA and induces cell death via a different mechanism than cisplatin. *Metallomics* **2013,** *5* (5), 514-523.
31. Diaz-Gomez, D. G.; Galindo-Murillo, R.; Cortes-Guzman, F., The Role of the DNA Backbone in Minor-Groove Ligand Binding. *Chemphyschem* **2017,** *18* (14), 1909-1915.

Highlights:

- A new insight of 2-phenyl-1-alkylaziridines and β-amino alcohols towards cancer cells
- Aziridine 5d was the most potent compound towards TNBC cell line
- β-amino alcohol 3f was the most active compound against MCF 7 cell line
- The compounds induced cell death most probably via an apoptotic pathway
- The compounds acted via a mechanism of action found on crescent-like shape molecules